Available online at www.elixirpublishers.com (Elixir International Journal)

Mechanical Engineering

Elixir Mech. Engg. 115 (2018) 49679-49685

ISSN: 2229-712X

Joint Conformity Resulting from Quadriceps Muscle and Ground Reaction Forces Influence Anterior Cruciate Ligament Response

Ariful Bhuiyan[1], Stephen Ekwaro-Osire[1], Sarhan M. Musa[2] and Mohammad Robiul Hossan[3]
[1]Department of Mechanical Engineering Texas Tech University, Lubbock, Texas 79409.
[2]Department of Engineering Technology Prairie View A&M University, Prairie View, Texas 77446.
[3]Department of Engineering and Physics University of Central Oklahoma, Edmond, OK 73034.

ARTICLE INFO

Article history:
Received: 13 December 2017;
Received in revised form:
20 January 2018;
Accepted: 30 January 2018;

Keywords
Anterior Cruciate Ligament (ACL),
Tibiofemoral joint,
Strain,
Injury,
Quadriceps Muscle Force (QMF) and
Ground Reaction Force (GRF).

ABSTRACT
Instrumented cadaveric knees were used to address the interaction between unopposed quadriceps muscle forces (QMF), ground reaction force (GRF), and strain in anterior cruciate ligament (ACL) through in-vitro simulation of a vertical jump-landing process. The objective of this research was to evaluate the effect of unopposed QMF, low knee flexion angle, joint conformity and constant GRF on the ACL strain. Fourteen cadaveric knees were mounted in a custom made dynamic loading simulator. The strain on the anteromedial bundle of the ACL was measured using a Differential Variable Reluctance Transducers (DVRT) sensor. Also, an I-Scan pressure transducer was used to measure the contact pressure and area in the tibiofemoral joint. During landing phase, the peak pressure on the lateral compartment is very high compared with the medial compartment. During landing phase, both the contact area and pressure increases in the tibiofemoral joint. The induced joint conformity caused by contact pressure has been justified. The results show that unopposed quadriceps muscle forces coupled with ground reaction force at low knee flexion angle cannot cause ACL injury. Joint compressive loads induced by large muscle forces and GRF introduces the joint conformity, and it produces the primary restraint against anterior tibial translation at low flexion angles.

1. Introduction

Anterior Cruciate Ligament (ACL) injury that occurs without physical contact with another person or object is referred as non-contact ACL injury (Ireland, Gaudette and Crook 1997). Approximately 70% to 80% of ACL injuries occur during non-contact sports events. These sports events involve different kinds of maneuvers such as sudden deceleration, an abrupt change in direction, or jump landing. These maneuvers are common in soccer, basketball, handball, and volleyball (Krosshaug et al. 2007, Boden et al. 2000, Boden et al. 2009). The growing number of people in sports, especially the increased participation of young females has resulted in an increase in the number of ACL injuries. Female ACLs are smaller compared with males; they do not grow in proportion to the body height and are of lower mechanical quality (Hashemi et al. 2011). It is reported that female athletes are 2-8 times more likely to sustain a non-contact ACL injury than males (Nagano et al. 2009, Ireland 2002).

Due to the advancement of the surgical techniques and rehabilitation, ACL surgery becomes a relatively routine procedure (Boden et al. 2000). However, recent research focuses more on the development of appropriate programs of intervention and prevention of non-contact ACL injury (Griffin et al. 2000). This requires better understanding the role of key factors such as quadriceps muscle force (QMF), ground reaction force (GRF) and knee flexion angle that contribute in ACL injury (Whiting and Zernicke 2008). The progress in the development of a matured prevention programs is somewhat slow due to lack of a well understood non-contact ACL injury mechanism (Bahr and Krosshaug 2005). Therefore, understanding injury mechanism is a central component of preventing non-contact ACL injuries (Bahr and Krosshaug 2005).

Several ACL injury mechanisms have been proposed to explain ACL injury mechanisms (Beynnon et al. 1995, Markolf et al. 1995, Fleming et al. 2001, Nunley et al. 2003, Arms et al. 1984). One of the most cited ACL injury mechanisms is quadriceps pull mechanisms (QPM). This mechanism stated that the contraction of quadriceps muscle force (QMF) results in a significant anterior proximal tibial translation at low knee flexion angles, and thus puts the ACL under tension (Beynnon et al. 1995, Markolf et al. 1995). Sometimes this mechanism is also termed as “anterior shear force mechanism.” Fleming et al. (Fleming et al. 2001), Markolf et al.(Markolf et al. 1995), Nunley et al. (Nunley et al. 2003) and Arms et al.(Arms et al. 1984) are among those researchers who studied rigorously on different aspects of QPM. Fleming et al. (Fleming et al. 2001) studied the effects of weight bearing and external loading of the tibia on the strain in ACL. A differential variable reluctance transducer (DVRT) was implanted on the anterior medial bundle of the ACL. Each subject’s leg was attached to a knee loading fixture. The knee loading fixture facilitated independent application of anterior-posterior directed shear force, valgus-varus moments and internal-external rotation moments to the tibia in the weight-bearing condition. The anterior shear force was applied to the proximal end of the tibia in 10 N increments from 0 N to 130 N.

Tele: 806 543 2007
E-mail address: prince95me@gmail.com

The valgus-varus moments and internal-external rotation were applied to the knee from -10 Nm to 10 Nm and from -9 Nm to 9 Nm in 1 Nm increments respectively. Their research reported that the strain in ACL was increased significantly as the anterior shear force at the proximal end of the tibia and the knee internal rotation moment were increased combinedly compared with any other combination. Markolf et al. (Markolf et al. 1995) investigated the effects of anterior shear force at the proximal end of tibia and knee valgus, varus, internal rotation and external rotational moments on the ACL loading in an in-vitro study. It was reported that the ACL loading was increased due to the combined effect of the anterior shear force, knee valgus-varus, and internal rotation moments at low knee flexion angle. The studies of Fleming et. al. (Beynnon et al. 1995, Fleming et al. 2001) and Markolf et al. (Markolf et al. 1995, Markolf et al. 2004) consistently showed that the anterior shear force at the proximal end of tibia generated from the quadriceps muscle force is a major contributor to ACL loading. As per QPM mechanism, an aggressive level of QMF can cause the substantial amount of proximal tibial translation. This translation of tibia put the ACL under tension; therefore, at some point, the ACL exceeds its failure strength.

However, there is an alternative mechanism of ACL injury available in the literature (Arms et al. 1984, Li et al. 1999, Yu and Garrett 2007, Draganich and Vahey 1990). The alternative mechanism proposed that a combination of strong QMF, low knee flexion angle, and a posteriorly directed GRF may induce tensile loading in ACL and cause ACL injury. A posteriorly directed GRF makes the knee flex at the time of landing. In parallel, the quadriceps load tries to increase to resist this excessive flexion of the knee (Arms et al. 1984). Consequently, this additional increase in the quadriceps force is believed to draw the proximal tibial to a significant amount, which induces extra loading in the ACL to a failure level. However, the literature based on QPM mechanism argued that at low flexion angles (less than15^{o}), hamstring co-contraction does not significantly reduce anterior tibial translation; therefore, the induced hamstring muscle force does not take any role in protecting the ACL (Li et al. 1999). On the other hand, the alternative mechanism argued that hamstring co-contraction will resist anterior tibial translation which is induced by the aggressive level of QMF.

Based on the literature review (Markolf et al. 1995, Markolf et al. 2004, Beynnon et al. 1995, Fleming et al. 2001, Nunley et al. 2003, Draganich and Vahey 1990), it is evident that the issues between the quadriceps pull mechanism (QPM) and alternative mechanism have not been resolved yet. The argument between these two groups is whether hamstring co-contraction is a factor in protecting ACL or not. In light of this situation, it requires more investigation to find out whether hamstring con-contraction or any other the factor(/s) is(/are) responsible for protecting or failing ACL for an unopposed QMF, low knee flexionand constant GRF. The objective of this research was to evaluate the effect of unopposed QMF, low knee flexion angle, joint conformity and constant GRF on the ACL strain. A detailed investigation of the effect of QMF, GRF on the ACL strain development and an evaluation of the articulation and interaction between femur and tibia along with their attached cartilages in knee joint kinematics has been presented.

2. Materials and Methods

2.1 Specimen Preparation

With the approval of Texas State Anatomical Board, 10 pairs (total 20 knees) fresh-frozen cadaver knees were obtained from the University of Texas Southwestern Willed Body Program and brought to Texas Tech University. The knees were kept frozen under -20^{0}C and thawed at room temperature for 10 hours prior to dissection. The knees were dissected to the capsule level just before the testing and 14 knees were selected for experiment based on the following criterion: (1) no ACL, PCL, LCL, and MCL injury, (2) ages were between 18 to 50 years, (3) no osteoarthritis, (4) no bone cancer, and (5) no reconstruction. Among those 14 knees, 8 bigger sized knees were also used to quantify the tibiofemoral contact pressure and area. A 75mm long section of 25mm wide woven nylon strapping was attached to the patella of each knee with annealed steel wire after dissection. Tissues and ligaments were kept moist by using 0.1N saline solution at 5 minutes interval throughout the experiment.

2.2 Experimental setup for measuring strain in ACL

The cadaver knee was placed in the custom made simulator shown in Figure 1. The details of the simulator can be found in (Hashemi et al. 2010).

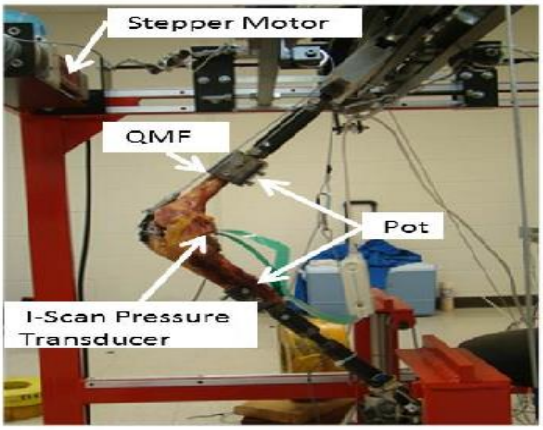

Figure 1. The dynamic simulator.The sagittal view of the Knee,right after applying the ground reaction force(GRF), showing the quadriceps cable (used to generate QMF), I-scan pressure transducer, stepper motor, and pot.

Briefly, the simulator was designed to apply predetermined sagittal plane muscle forces to the loaded knee by the stepper winch (resolution 8-25 micrometer). The steel actuation cables (McMaster-Carr, Aurora, OH) of 3.2 diameters was used to attach the stepper winches to the cadaver knees. A Differential Variable Reluctance Transducers (DVRTs) of 3 mm stroke length was mounted on the anteromedial bundle of the ACL to record its change in length using proximal and distal barbed pins. Care was taken to ensure that the DVRT barbs were not inserted too close to tibial insertion to avoid the interaction of the barbs with the underlying bone. DVRTs have been extensively used both in vivo and in vitro to measure strain in the ACL (Hashemi et al. 2010, Withrow et al. 2006). The ACL is strained at the time of DVRT insertion but to a very lower scale. This setting is sufficient to measure in-situ strain in the ACL in between 10% to 20% (Hashemi et al. 2010). The sensor was calibrated to measure inter-barb lengths of 9-12 mm. The load cell measurements were calibrated, using NI Labview 8.2 software and a USB multifunction DAQ (NI USB-6009, National Instruments, and Austin, TX)

The knees were installed in the dynamic simulator after the dissection. The knee was positioned at around 20^o flexion angle. In this vitro study, 5 different QMFs: 25N, 75N, 175N, 200N and 300N were applied to each knee with 5 minutes interval between QMFs. After applying each QMF, the ACL pre-strain data was recorded, and then, a ground reaction force (GRF) was applied to each knee in order to get the total strain (total strain = pre-strain + landing strain) value. The GRF was produced by a carriage mounted drop weight (7 kg). The height of the drop was fixed at 60cm. In order to get pre- and total strain for each loading combination, 28 independent tests (14 knees) were conducted, resulting in a total 140 sets of data (14 knees x (5+5) set of data= total 140 set of data) as shown in Table 1.

Table l. The total Experimental set od data for this research.

Total Number of knees	QMF	GRF	Set of data	description
14	5	0	14x5=70	Each knee was loaded with 5 different QMF for measuring the pre strain in ACL
14	5	1	14x5=70	Each knee was loaded with 5 different QMF couple with GRF each time for measuring the total strain in ACL
9	5	0	9x(5+5+5)=135	Each knee was loaded with three cycle of same QMF to measuring the peak contact pressure and contact area in the tibiofemoral joint prior to landing phase.
9	5	1	9x5=45	Each knee was loaded with QMF coupled with GRF to measuring the peak contact pressure and contact area in the tibiofemoral joint during the landing Phase

2.3 Experimental setup for measuring contact pressure and area

A separate computerized, real-time, thin-film pressure transducer methods (I-Scan model 4000) was used to capture the contact pressure and area data from the tibiofemoral joint. The pressure transducers are more reliable and reproducible as compared to Fuji pressure-sensitive film (Harris et al. 1999). The I-Scan sensor has two 9.2 cm^2 sensing arrays, each with 2288 sensing elements. The I-Scan sensors are made with a dimensionally stable polyester substrate so that it can easily be used on a curved surface. It responds to the individual local normal forces, and the software sums these forces. The sensor was conditioned with cadaveric knees by subjecting it to three cycles of loading from 500N (held for 30 s) to 10N (held for 30 s) for each cadaveric knee. Each knee was loaded to 500N and it was ensured that the footprint of the tibiofemoral contact point fell completely within the margins of the sensor, and then backed off to a preload of 10N. The sensor was then equilibrated and calibrated at 300N.

Eight bigger sized knees were selected to collect contact pressure and area data from the lateral and medial compartments of those knees. After completion of the experiment to measure the pre and total strain, the DVRT was taken out from the ACL, and the I-Scan (model 4000) was inserted into the tibiofemoral joint from the posterior side of the knee to measure the contact pressure and area. The overall experimental setup and knee loading procedures were similar as described in the previous section for measuring ACL strain. A course of QMFs: 25N, 75N, 175N, 200N, and 300N were applied to each installed knee with 5-minute intervals. The static peak contact pressure and the area were recorded and repeated for 3 times to get an average value. After applying each QMF, a ground reaction force (GRF) was applied to each knee in order to again get the final contact pressure and area. The details of the total set of experiments and the set of data are presented in Table1.

There are three possible sources of errors at the time of conducting this kind of experiment: (1) humidity (Ateshian et al. 1994, Hull and Howell 1997) (2) temperature (Ateshian et al. 1994), and (3) shear artifact (Hull and Howell 1997). All the tests for a knee were conducted on the same day to control for temperature and humidity. In addition, the knee joint space was created to avoid shear artifacts when placing the film into the joint. All instruments used in these experiments were connected to NI-USB data acquisition device (National Instruments, Austin, TX). Spectral analysis of all data channels was performed and showed that frequency of response of all channels was below 150 Hz. Therefore, the sampling rate was set at 1 kHz, which is perfect as per the Shannon-Nyquist sampling theorem. In addition, all data channels were low-pass filtered at 400 Hz.

Results and Discussions

In this studies, 5 independent static QMFs (25N, 75N, 175N, 200N, and 300N) were applied to each knee with a knee flexion angle of 20°. No ACL failure was observed after applying these static QMFs. It was reported that the pre-strain in ACL reaches to 3.5 % just before landing (Cerulli et al. 2003). It would require 550 N QMF in in-vivo experiment to generate similar ACL strain. Therefore, the maximum QMF 300N used in this study is within the limit. The pre-strain in ACL ranged from slack to 1.95%. In all 14 knees, there was a positive correlation between QMF and ACL pre-strain as presented in Table 2. Similar observations were made by Li et al. (Li et al. 1999) during the research work.

Table 2. Correlation statistics for pre-strain versus QMFs

Knees	Correlation statistics (or) pre-strain
K1	0.910
K2	0.935
K3	0.938
K4	0.923
K5	0.911
K6	0.927
K7	0.851
K8	0.935
K9	0.924
K10	0.893
K11	0.857
K12	0.946
K13	0.800
K14	0.820

The variation of pre-strain and total strain (pre-strain and landing strain) against QMFs are shown in Figure 2. It shows that the pre-strain is around 0.25% when the QMF is 25 N as seen in Figure 2a. The pre-strain gradually increases along with the increased QMF. The highest pre-strain was found to be 1.95% for the highest QMF of 300 N. It was observed that the tibia moved anteriorly relative to the femur as the QMF was increased. This puts the ACL in tension and pre-strain increase as the QMF increases. Therefore large QMF prior to landing yields large pre-strains in ACL and similar observation is reported in (Hashemi et al. 2010) as well.

However, the total strain (pre-strain + landing strain) did not vary much with the increasing QMF as seen in Figure 2b. This implies that 1.) When the QMF is low, the pre-strain in ACL is low, and the induced landing strain in the ACL is high, and 2.) When the QMF is high, the pre-strain in ACL is high, and the induced landing strain in the ACL is low. Observations consistent with this were also made by (Hashemi et al. 2010).

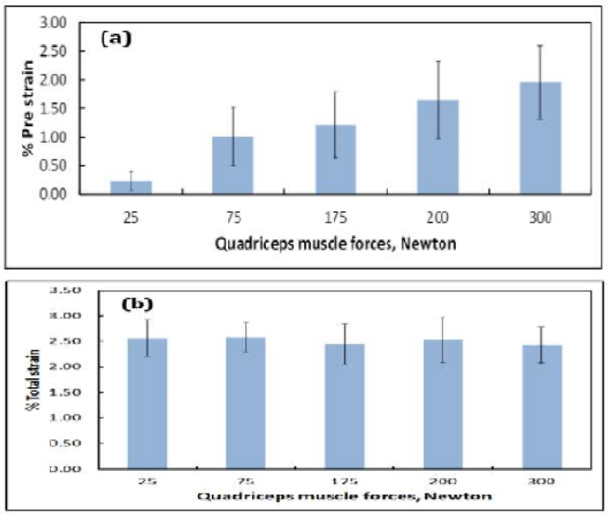

Figure 2. The variation of ACL strain against different QMFs for a pool all knees.a)% pre-strain versus QMFs. The pre-strain is the strain measured prior to landing phase.b) % total strain versus QMFs. The total strain remains around 2.50% along with different QMFs.

During landing phase, the ground reaction force (GRF) takes approximately 10ms to reach its peak value, and it starts to fall off from the peak point immediately as shown in Figure 3. GRF reaches to zero value at around 45ms. The GRF was simulated by dropping of carriage weight 7 kg from a height of 60 cm, while the maximum static quadriceps force, 175N was generated with the help of a stepper motor. Measurements are normalized to their peak values. The input QMF starts with approximately 0.5, which represents the applied static QMF of 175N (normalized by 350N) prior to landing time (at the starting point of the GRF). Figure 3 also shows that the static input of QMF starts increasing right after the knee gets coupled with GRF. Similar kind of kind of increasing pattern of QMFs during the time of applying GRF was observed for other four pre-applied QMFs of 25N, 75N, 200N, and 300N. A sudden stretch of a pre-tensioned quadriceps muscle caused by knee flexion elicits a large increase in quadriceps force.

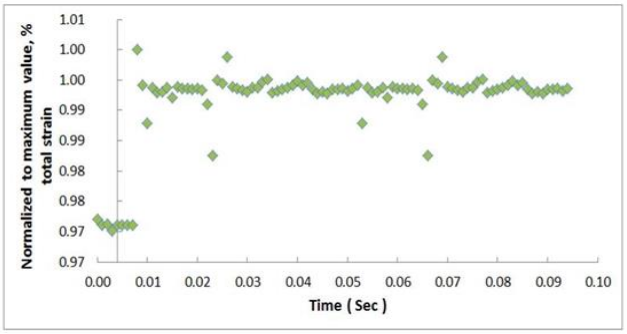

Figure 3. Response of an ACL from a knee (Exp sub #60103L): The total strain of the ACL. Measurements are normalized to their peak values.

It happens because of its inherent dynamic resistance to stretch caused by its stiffness and damping properties. Both stiffness and damping properties are known to be proportional to muscle force (Withrow et al. 2006). Figure 4 shows the total ACL strain response from a knee. The experiment was able to capture the signature of the peak total strain and GRF as shown in Figure 3 and Figure 4.

In this experiment, no hamstring force was applied to the knee. The total strain for all cases was around 2.5%, which is below than the ACL failure strength. Therefore, the total strain pattern, which remains at a constant level regardless of the QMF, indicate that co-contraction of hamstring muscles does not contribute to protecting ACL. Next, we evaluate the articulation and interaction between femur and tibia along with their attached cartilages in knee joint kinematics.

Figure 5 shows the contact mapping of pressure distribution on the lateral and medial compartment of a knee for before and after landing condition. Figure 5 (a- e) shows the peak contact pressure and its associated contact area on the lateral and medial compartment while the knee is under the QMFs of 25N, 75N, 175N, 200N, and 300N respectively. The peak contact pressure for QMF 25N is 0.303 MPa and it is located in the medial compartment. The peak contact increases for all other QMFs. However the location of the peak contact pressure transferred to the lateral compartment for QMFs above 75 N as seen in Figure 5 (a-e). The shifting of the peak contact stress from medial to lateral compartment was also observed for all other seven cadaveric knees for the quadriceps forces above 75N. The internal tibial rotation for all other seven knees was observed at the time of experiments.

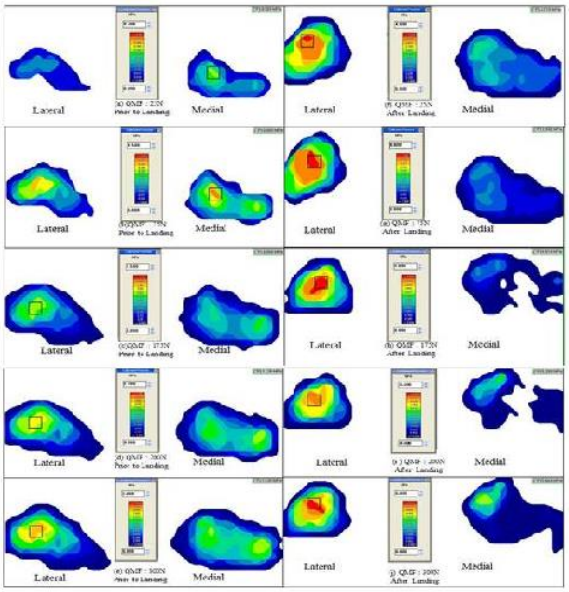

Figure 4. Peak contact pressure (MPa) and its associated area details (mm^2) for (a-e) before landing and (f-j) after landing.

Figure 5 (f-j) shows the peak contact pressure and its associated contact area on the lateral and medial compartment of a knee after landing time. The peak contact pressure for QMF 25 N coupled with GRF is 3.719MPa, and it is located in the lateral compartment. Both the peak contact area and pressure keeps on increasing for the rest of the four set of loadings. The location of the peak contact pressure remains in the lateral compartment for each of this five loading conditions Figure 5(f-j). The results show that the localized lateral contact pressure tries to spread out along the anterior-medial path, which indicates that the tibia tries to rotate internally. The internal tibial rotation was also observed during experiments and thus it causes tension in the ACL.

Similar observations were also reported by (Hashemi et al. 2010, Markolf et al. 2004, Harris et al. 1999). To the best of our knowledge, this is the first time that this research reports about how the tibiofemoral joint contact pressure and contact area contours respond due to the interaction between the femur and tibial cartilages.

The peak contact pressure, area and percentage change in peak pressure and contact area for before and after landing are shown in Figure 6 as a function of various QMFs. The results show that the peak contact pressure increases along with the increasing QMFs (Figure 6a). The peak contact pressure increasing pattern is also observed during the landing phase Figure 6 (b). Figure 6 (c) shows that the maximum peak contact pressure percentage increase before and after landing happens when the QMF is low, and the value is 1250%; the minimum peak contact pressure percentage increase happens when the QMF is high, and the value is around 20%. The same kind of pattern is also observed for the contact area, i.e, the maximum peak contact area increases happen for both prior to landing and during landing phase Figure 6 (d) and Figure 6 (e). It also shows that the maximum peak contact area percentage increase happens when the QMF is low, and the value is 360%; the minimum peak contact pressure percentage increase happens when the QMF is high, and the value is around 5% (Figure 6f).

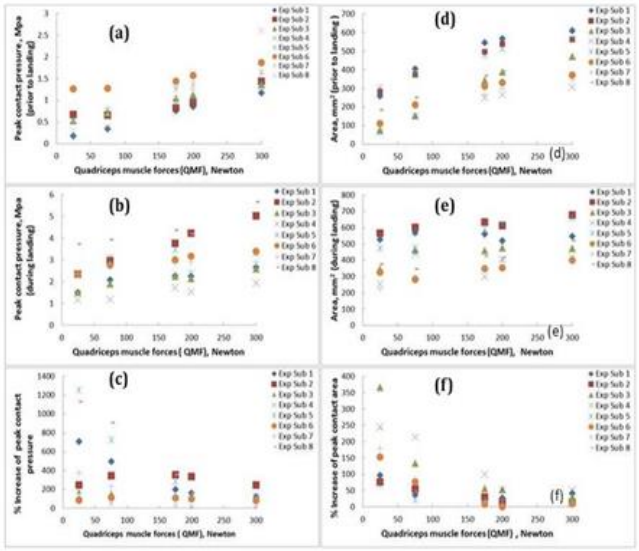

Figure 5. a) For various QMFs, Peak contact pressure prior to landing
b) Peak contact pressure during landing
c) Percentage increase in peak contact pressure prior to land during landing in MPa
d) Peak contact area prior to landing
e) Peak contact area during landing and
f) percentage increase in contact area prior ta and during landing in mm^2.

Considering all the parameters that were studied in this research, it shows that ACL, contact pressure, and area are increased with the QMFs. Similarly when unopposed QMF is coupled with GRF, the landing strain, peak contact pressure and area increases with increasing QMF.

However, the total strain in ACL always remains at around 2.5% which is below ACL failure value. It indicates that the increased contact area and pressure may put a restriction on tibial anterior movement. Figure 7 shows the rising time history of the peak contact pressure and area for the experimental subject (Exp Sub) #1. All the measurements are normalized to their peak values. The GRF was normalized with the value which is due to the dropping weight 7 kg from a height of 60 cm; The QMF was normalized with the maximum quadriceps force, 175N.

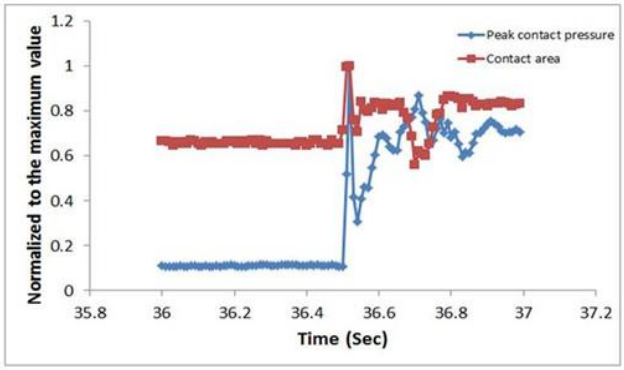

Figure 6. Time to reach the peak contact pressure and area for the Exp sub#1.

The maximum peak contact pressure was 3.932MPa, and the maximum contact area was 347mm2. Peak contact pressure takes approximately 14 to 16ms to reach its peak value whereas the corresponding contact area takes around 16 to 20ms to reach its peak value. It is also shown Figure 4 that the total strain reaches out to its maximum value within the 5 to 7ms. Hence it is not necessary for the contact pressure and area to reach out to their peak value to lock the knees. Rather the joint compressive loads induced by large muscle forces and GRF introduces the joint conformity, and this joint conformity produces the primary restraint against anterior tibial translation at low flexion angles.

Conclusions

This paper presents a comprehensive in-vitro experimental investigation to evaluate the effect of unopposed quadriceps muscle forces (QMF) and ground reaction force (GRF) on the strain development of anterior cruciate ligament (ACL). The results show that the total ACL strain remains almost same (2.5%) regardless of the QMFs for a constant GRF. However, the pre-strain in ACL increases with the increase of unopposed QMFs. The strain does not exceed the failure strain in either in pre-strain or total strain values. Therefore based on the experimental results it can be concluded that the quadriceps muscle force (not considering the hamstring or other muscle forces) coupled with a GRF cannot cause ACL injury during the landing phase provided the initial flexion angle is around 20°. It is justified that joint compressive loads induced by large muscle forces and GRF introduce the joint conformity, and this joint conformity produces the primary restraint against anterior tibial translation at low flexion angles. Because of the joint conformity resulting from QMF and GRF, the ACL strain remains constant.

Acknowledgement:

Dr. Hashemi (Florida Atlantic University) and Dr. Naveen Chandrashekar (University of Waterloo) are recognized for sharing their equipments and instruments for this research.

References

Arms, S. W., M. H. Pope, R. J. Johnson, R. A. Fischer, I. Arvidsson & E. Eriksson (1984) The biomechanics of anterior cruciate ligament rehabilitation and reconstruction. *The American journal of sports medicine,* 12**,** 8-18.

Ateshian, G., S. Kwak, L. J. Soslowsky & V. Mow (1994) A stereophotogrammetric method for determining in situ contact areas in diarthrodial joints, and a comparison with other methods. *Journal of biomechanics,* 27**,** 111-124.

Bahr, R. & T. Krosshaug (2005) Understanding injury mechanisms: a key component of preventing injuries in sport. *British journal of sports medicine,* 39**,** 324-329.

Beynnon, B. D., B. C. Fleming, R. J. Johnson, C. E. Nichols, P. A. Renström & M. H. Pope (1995) Anterior cruciate ligament strain behavior during rehabilitation exercises in vivo. *The American Journal of Sports Medicine,* 23**,** 24-34.

Boden, B. P., G. S. Dean, J. A. Feagin & W. E. Garrett (2000) Mechanisms of anterior cruciate ligament injury. *Orthopedics,* 23**,** 573-578.

Boden, B. P., J. S. Torg, S. B. Knowles & T. E. Hewett (2009) Video analysis of anterior cruciate ligament injury abnormalities in hip and ankle kinematics. *The American journal of sports medicine,* 37**,** 252-259.

Cerulli, G., D. Benoit, M. Lamontagne, A. Caraffa & A. Liti (2003) In vivo anterior cruciate ligament strain behaviour during a rapid deceleration movement: case report. *Knee Surgery, Sports Traumatology, Arthroscopy,* 11**,** 307-311.

Draganich, L. & J. Vahey (1990) An in vitro study of anterior cruciate ligament strain induced by quadriceps and hamstrings forces. *Journal of Orthopaedic Research,* 8**,** 57-63.

Fleming, B. C., P. A. Renstrom, B. D. Beynnon, B. Engstrom, G. D. Peura, G. J. Badger & R. J. Johnson (2001) The effect of weightbearing and external loading on anterior cruciate ligament strain. *Journal of biomechanics,* 34**,** 163-170.

Griffin, L. Y., J. Agel, M. J. Albohm, E. A. Arendt, R. W. Dick, W. E. Garrett, J. G. Garrick, T. E. Hewett, L. Huston & M. L. Ireland (2000) Noncontact anterior cruciate ligament injuries: risk factors and prevention strategies. *Journal of the American Academy of Orthopaedic Surgeons,* 8**,** 141-150.

Harris, M., P. Morberg, W. Bruce & W. Walsh (1999) An improved method for measuring tibiofemoral contact areas in total knee arthroplasty: a comparison of K-scan sensor and Fuji film. *Journal of biomechanics,* 32**,** 951-958.

Hashemi, J., R. Breighner, T.-H. Jang, N. Chandrashekar, S. Ekwaro-Osire & J. R. Slauterbeck (2010) Increasing pre-activation of the quadriceps muscle protects the anterior cruciate ligament during the landing phase of a jump: an in vitro simulation. *The knee,* 17**,** 235-241.

Hashemi, J., H. Mansouri, N. Chandrashekar, J. R. Slauterbeck, D. M. Hardy & B. D. Beynnon (2011) Age, sex, body anthropometry, and ACL size predict the structural properties of the human anterior cruciate ligament. *Journal of orthopaedic research,* 29**,** 993-1001.

Hull, M. & S. Howell (1997) An in vitro osteotomy method to expose the medial compartment of the human knee. *Journal of biomechanical engineering,* 119**,** 379.

Ireland, M. L. (2002) The female ACL: why is it more prone to injury? *Orthopedic Clinics of North America,* 33**,** 637-651.

Ireland, M. L., M. Gaudette & S. Crook (1997) ACL injuries in the female athlete. *Journal of Sport Rehabilitation,* 6**,** 97-110.

Krosshaug, T., A. Nakamae, B. P. Boden, L. Engebretsen, G. Smith, J. R. Slauterbeck, T. E. Hewett & R. Bahr (2007) Mechanisms of anterior cruciate ligament injury in basketball video analysis of 39 cases. *The American journal of sports medicine,* 35**,** 359-367.

Li, G., T. Rudy, M. Sakane, A. Kanamori, C. Ma & S.-Y. Woo (1999) The importance of quadriceps and hamstring muscle loading on knee kinematics and in-situ forces in the ACL. *Journal of biomechanics,* 32**,** 395-400.

Markolf, K. L., D. M. Burchfield, M. M. Shapiro, M. F. Shepard, G. A. Finerman & J. L. Slauterbeck (1995) Combined knee loading states that generate high anterior cruciate ligament forces. *Journal of Orthopaedic Research,* 13**,** 930-935.

Markolf, K. L., G. O'Neill, S. R. Jackson & D. R. McAllister (2004) Effects of applied quadriceps and hamstrings muscle loads on forces in the anterior and posterior cruciate ligaments. *The American journal of sports medicine,* 32**,** 1144-1149.

Nagano, Y., H. Ida, M. Akai & T. Fukubayashi (2009) Biomechanical characteristics of the knee joint in female athletes during tasks associated with anterior cruciate ligament injury. *The Knee,* 16**,** 153-158.

Nunley, R. M., D. Wright, J. B. Renner, B. Yu & W. E. Garrett Jr (2003) Gender comparison of patellar tendon tibial shaft angle with weight bearing. *Research in Sports Medicine,* 11**,** 173-185.

Whiting, W. C. & R. F. Zernicke. 2008. *Biomechanics of musculoskeletal injury*. Human Kinetics.

Withrow, T. J., L. J. Huston, E. M. Wojtys & J. A. Ashton-Miller (2006) The relationship between quadriceps muscle force, knee flexion, and anterior cruciate ligament strain in an in vitro simulated jump landing. *The American journal of sports medicine,* 34**,** 269-274.

Yu, B. & W. E. Garrett (2007) Mechanisms of non-contact ACL injuries. *British journal of sports medicine,* 41**,** i47-i51.

Ariful I. Bhuiyan received his Ph.D. in Mechanical Engineering from Texas Tech University in 2013. Dr. Bhuiyan has an extensive experience on system engineering, bioengineering, sensor and new product development. His current research interests include new product development, data minining, network and database securiy.

Dr. Stephen Ekwaro-Osire is a full professor in the Department of Mechanical Engineering, and a licensed professional engineer in the state of Texas. Dr. Ekwaro-Osire most recently served as Associate Dean of Research and Graduate Programs. Prior to that he was the acting chair of the Department of Mechanical Engineering, and the interim chair of the Department of Industrial Engineering. Before that, he served as the director of the undergraduate program, and director of the graduate program and graduate advisor in the Department of Mechanical Engineering. He was recently a Fulbright Scholar.Dr. Ekwaro-Osire's research interests are engineering design, wind energy, vibrations, and orthopedic biomechanics. As a Summer Faculty Fellow, he conducted research at NASA Glenn Research Center and the Air Force Research Laboratory. His research has been funded by the National Science Foundation, the Department of Energy, the state of Texas, and industry. He has 113 refereed papers in conference proceedings, 47 refereed archival papers in scientific journals, 12 book chapters, and 2 books. In addition to other papers, he is a holder of 1 provisional patent. He has supervised and graduated 32 doctoral and master's students. He has received numerous awards and recognitions for his contributions in teaching, research, and service. Dr. Ekwaro-Osire is a member of Texas Tech University's Teaching Academy, which promotes and recognizes teaching excellence at the university. He is an active member of the

American Society for Engineering Education, the American Society of Mechanical Engineers, the Society for Design and Process Science, the American Society of Biomechanics, and the Society for Experimental Mechanics.

Sarhan M. Musa is a professor in the Department of Engineering Technology at Prairie View A&M University, Texas. He received his Ph.D. in Electrical Engineering from the City University of New York in 2001. Professor Musa has been the founder and director of Prairie View Networking Academy (PVNA), Texas, since 2004. He is a leading researcher at Center of Excellence of Communication Systems Technology Research (CECSTR) and SECURE Center of Excellence at Prairie View A&M University, Texas. Dr. Musa is LTD Sprint and Boeing Welliver Fellow. Professor Musa has written more than a dozen books on various areas of study in Mathematics and Engineering. His current research interests include computational electromagnetic, computational nanotechnology, photonics, imaging and spectroscopy, cybersecurity, Internet of things, big data analytics, and cloud computing.

Dr. Mohammad Robiul ("Robi") Hossan joined as an Assistant Professor of Mechanical Engineering in August 2013. He received his PhD from Washington State University in July 2013. His research focuses on: electrokinetics in microfluidic devices for biomedical applications, electromagnetic heating and development of numerical methods for particle transport in microfluidics. Dr. Hossan regularly publishes his research in international journals and conference proceedings. In his PhD research, he developed hybrid numerical model for dielectrophoretic particle transport, integrated microfluidic device for separation and detection of cardiac biomarker proteins, and theoretical model for microwave heating. He has experience in cleanroom processes for micro/nano fabrication of microfluidic devices. Dr. Hossan is actively involved with American Society of Mechanical Engineers (ASME), organizing national and international conferences and serving as reviewers for numerous journals and conference proceedings.